

---

# A Proposal for New Algorithm that Defines Gait-Induced Acceleration and Gait Cycle in Daily Parkinsonian Gait Disorders

---

Masahiko Suzuki, Makiko Yogo, Masayo Morita, Hiroo Terashi, Mutsumi Iijima, Mitsuru Yoneyama, Masato Takada, Hiroya Utsumi, Yasuyuki Okuma, Akito Hayashi, Satoshi Orimo and Hiroshi Mitoma

Additional information is available at the end of the chapter

<http://dx.doi.org/10.5772/intechopen.75483>

---

## Abstract

We developed a new device, the portable gait rhythmogram (PGR), to record up to 70 hrs of movement-induced accelerations. Acceleration values induced by various movements, averaged every 10 min, showed gamma distribution, and the mean value of this distribution was used as an index of the amount of overall movements. Furthermore, the PGR algorithm can specify gait-induced accelerations using the pattern-matching method. Analysis of the relationship between gait-induced accelerations and gait cycle duration makes it possible to quantify Parkinson's disease (PD)-specific pathophysiological mechanisms underlying gait disorders. Patients with PD showed the following disease-specific patterns: (1) reduced amount of overall movements and (2) low amplitude of gait-induced accelerations in the early stages of the disease, which was compensated by fast stepping. Loss of compensation was associated with slow stepping gait, (3) narrow range of gait-induced acceleration amplitude and gait cycle duration, suggesting monotony, and (4) evident motor fluctuations during the day by tracing changes in the above two parameters. Prominent motor fluctuation was associated with frequent switching between slow stepping mode and active mode. These findings suggest that monitoring various movement- and gait-induced accelerations allows the detection of specific changes in PD. We conclude that continuous long-term monitoring of these parameters can provide accurate quantitative assessment of parkinsonian clinical motor signs.

**Keywords:** portable gait rhythmogram, gait disorder, gait analysis, wearable device, Parkinson's disease

---

# 1. Introduction

## 1.1. Why are wearable monitors necessary in clinical management?

Patients with various neurological and musculoskeletal conditions present with a variety of gait abnormalities. Parkinson's disease (PD), parkinsonism-related diseases, and cerebellar ataxias show clinically specific features of gait disorders [1–10]. PD is characterized by poverty of movements (akinesia) and slowness/smallness of executed movement (bradykinesia) [1–10]. Parkinsonian gait disorders are assessed by using clinical score (Unified Parkinson's Disease Rating Scale (UPDRS)) [11], Timed Up and Go testing [12], and gait analysis on short-distance walking [10, 13]. However, these methods have limitations regarding exact assessment. First, there are dispersions in estimation on UPDRS depending on the examiners. Second, information outside the hospital examination rooms is lacking. Finally, gait analysis on short-distance walking can be easily influenced by emotional stress caused by increased attention [10, 13].

Proper assessment of the characteristic features of each gait disorder should satisfy two conditions: (1) measure specific kinematic and temporal parameters that reflect deficits in particular neural circuitry [13] and (2) measure voluntary control of gait movements continuously over a long period of time during activities of daily living (ADL) [1, 5–8]. For these reasons, many types of wearable devices that monitor activities including gait have been proposed (see **Table 1**) [14–24]. Maetzler et al. [14] proposed the following clinical features as targets for wearable

Types of sensors	
Devices that mainly monitor overall activities	
TricTrac RT3 [9, 20]	Accelerometer- and gyroscope-mounted sensor
Devices that mainly monitor gait disorders	
Step watch [19, 20]	Specific ankle-worn microprocessor-based step counter
DynaPort [19, 20]	Accelerometer-mounted sensor attached on the trunk
Devices that monitor changes in overall activities and gait disorders	
Mobility lab [21, 22]	Accelerometer- and gyroscope-mounted sensor attached on the limbs and trunk
Physiolog [23]	Accelerometer-, gyroscope-, and barometric pressure-mounted sensors attached on the limbs and trunk
AX3 [24]	Accelerometer-mounted sensor attached on the limbs or trunk

**Table 1.** Features of currently available wearable devices.

devices: (1) motor disabilities, including axial disability (gait and transfer deficits, freezing of gait, imbalance, and frequent falling), bradykinesia in the distal limb, dyskinesia, resting tremor, dysarthria, and secondary low activity, and (2) non-motor clinical features, which include sleep disturbance and autonomic dysfunction [14]. So far, gait-induced accelerations and angular velocities have been used to assess gait akinesia and bradykinesia in PD [14, 25].

## **1.2. Advantages of accelerometer-mounted wearing device**

Accelerometer-mounted devices were originally developed to record all movement-induced accelerations [26–29]. Since acceleration-mounted sensors have advantages in quantitative assessment of PD-specific changes underlying PD gait disorders, among other types of sensors [14, 15], acceleration signals have recently been analyzed [30–36].

Especially, a series of studies by Weiss and colleagues have clarified the clinical validity of quantification of gait-induced accelerations [12, 37–40]. They calculated the gait cycle time and the step-to-step variability in PD patients [37–40]. Importantly, the step-to-step variability was higher in fallers than non-fallers [37, 38] and in freezers than nonfreezers [39]. They also showed that the amplitudes of gait-induced accelerations can be good indices for gait disorders [37–40]. These studies suggest that quantification of gait-induced accelerations, cycles, and amplitudes can identify PD-specific changes in gait control. Thus, further development of improved algorithm is desirable.

## **1.3. Proposal of a new algorithm: relationship between gait-induced acceleration and gait cycle duration**

In order to assess physiologically gait akinesia/bradykinesia in PD, we have developed a new system (the portable gait rhythmogram (PGR)) for long-term monitoring of gait-induced accelerations during walking and daily routine activity. This system consists of two components: the first component is a wearable device with an acceleration sensor, and the second one is an automatic gait detection algorithm. Gait-induced accelerations are deduced from limb and trunk movements using a mathematical algorithm known as the “pattern-matching method” [41–54]. Thus, the PGR can quantitatively identify various movement-induced accelerations and gait-induced accelerations, respectively.

In a series of publications, we described the motor signs of patients with PD recorded by the PGR [41–54]. Mathematical analysis of various movement-induced accelerations allowed us to quantify poverty of movements. Furthermore, examination of gait-induced accelerations clarified two major features of parkinsonian gait: (1) disabilities in force generation and rhythm setting and (2) loss of dynamic modulation of the force and rhythm depending on the context. By tracing gait fluctuations, it was possible to trace the time and degree of motor fluctuation.

The present article is a review of our published data on the PGR and gait disorders [41–54] and proposes a new algorithm that defines the relationship between gait-induced acceleration and gait cycle duration so as to quantify comprehensively PD-specific pathophysiological mechanisms underlying PD gait disorders.

## 2. Identification of gait-induced accelerations using pattern-matching method and analysis of gait force-rhythm relationship

### 2.1. Monitoring of motion-induced acceleration

Acceleration signals were measured by a portable PGR equipped with a triaxial accelerometer (Mimamori-gait system, LSI Medience Corporation: size, 75 mm × 50 mm × 20 mm; weight, 120 g) (Figure 1A) [41–54]. The sensor is sensitive not only to dynamic acceleration associated with rapid body movements but also to those with static acceleration due to gravity. The PGR was secured with a fixation belt to the front center of the subject's waist (predefined position) at the start of the study. The subject was instructed to go about her/his activities in free-living environment for a period of 24 hrs with the device attached at all times except when changing clothes or taking a bath. When standing in the anatomical position, the orientation of the three acceleration axes— $x$ ,  $y$ , and  $z$ —was medial/lateral, vertical, and anterior/posterior, respectively. The rhythmogram measured three-dimensional accelerations ( $a_x$ ,  $a_y$ ,  $a_z$ ) associated with limb and trunk movements, as well as those induced by step-in and kickoff during gait. Data were collected at a sampling rate ( $\Delta t$ ) of 10 ms and stored on a Secure Digital card inserted into the device for later analysis using a custom-made software program. A fully charged PGR can achieve 70 hrs of continuous recording.

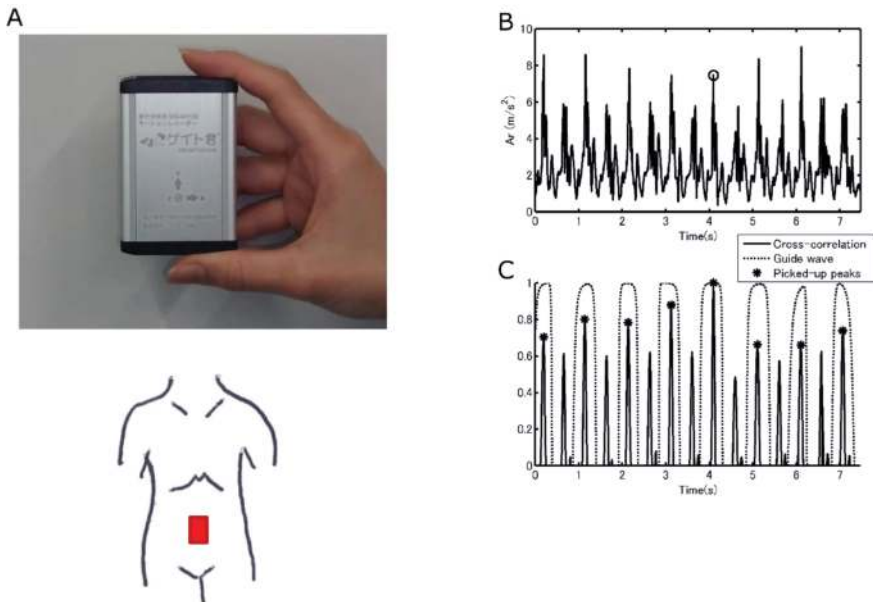


**Figure 1.** The portable gait rhythmogram device and illustration of the sensor placements (A), Examples of total acceleration signal during walking (B), and corresponding cross correlation (solid line), guide wave (dotted line), and picked-up peaks (asterisk) (C).

## 2.2. Identification of acceleration induced by gait motion

### 2.2.1. Overview of analytical tools for gait detection

For the analysis of gait characteristics from the three-dimensional acceleration signal, it is important to correctly extract the timing of every stride event during walking (hereafter referred to as stride peak or gait peak). Several basic gait features can be utilized for this purpose. First, walking is a repeated body movement and therefore is accompanied by rhythmic acceleration patterns. This rhythmicity can be captured by the conventional template-matching method [41–44]. Details of the mathematical calculations were reported in our previous methodological articles [42–44, 50]. **Figure 2** shows a summary diagram of the algorithm.

In the present study, the recorded acceleration signal is filtered by a high-pass filter  $sT_F / (1 + sT_F)$  to remove slow trends caused by body inclination. The time constant  $T_F$  is set at 0.7 sec. From the filtered signal, we choose a three-dimensional (3D) template wave composed of  $p$  consecutive points:

$$[Ax(t + i\Delta t) \quad Ay(t + i\Delta t) \quad Az(t + i\Delta t)] \quad (1)$$

where  $i = 0, 1, \dots, p-1$ .

Then, the normalized cross correlation between this wave and an arbitrary signal segment of the same length as the template with a time shift of  $T$  is obtained by the following equation:

$$\frac{\frac{1}{p} \sum_{i=0}^{p-1} [Ax(t + i\Delta t)Ax(t + i\Delta t + T) + Ay(t + i\Delta t)Ay(t + i\Delta t + T) + Az(t + i\Delta t)Az(t + i\Delta t + T)]}{\left\{ \frac{1}{p} \sum_{i=0}^{p-1} [Ax(t + i\Delta t)^2 + Ay(t + i\Delta t)^2 + Az(t + i\Delta t)^2] \right\}^{\frac{1}{2}} \left\{ \frac{1}{p} \sum_{i=1}^p [Ax(t + i\Delta t + T)^2 + Ay(t + i\Delta t + T)^2 + Az(t + i\Delta t + T)^2] \right\}^{\frac{1}{2}}} \quad (2)$$

Here, the average value is subtracted from each acceleration component beforehand. The normalized cross correlation characterizes the similarity between two signal segments (therefore, the rhythmicity of the signal), offering the basis of self-adaptive algorithm of automatic gait peak detection [41–44]. Moreover, this value is a robust measure because it is rather insensitive to the manner of setting the coordinate system. This feature is especially useful in the analysis of long-term acceleration data, since the position or orientation of the device might be altered from the predefined one during the day; for example, it sometimes occurs that the device is worn upside down and/or back to front after the patient changes clothes.

We also paid attention to another important feature of gait: biphasicity vs. monophasicity. This means that, during one gait cycle, both vertical and anterior/posterior accelerations change in a biphasic manner, that is, a similar pattern is repeated twice per cycle, while medial/lateral acceleration shows a monophasic pattern. The biphasicity/monophasicity inherent in human gait helps to identify correct stride peaks with high precision as described below.

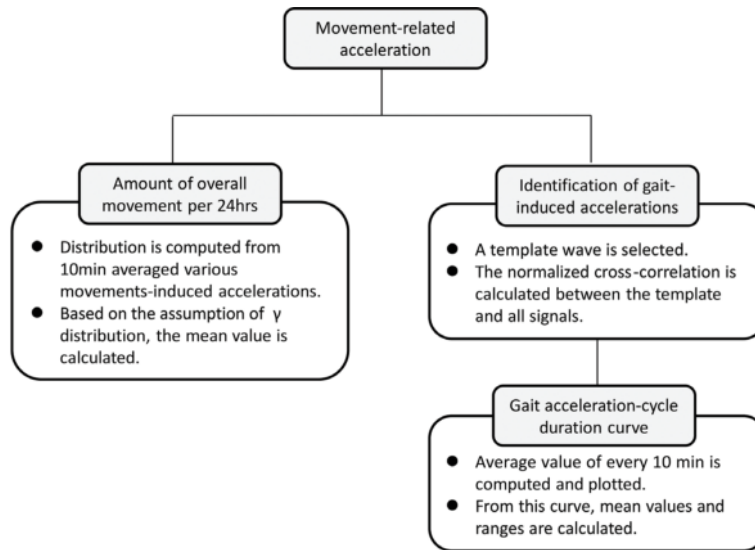


**Figure 2.** Diagram of the algorithm using the pattern-matching method and analysis of the relationship between gait force and rhythm.

### 2.2.2. Estimation of continuously walking region

Possible walking regions with stride cycle <2 sec are estimated from the whole time series by the following procedure:

- Total acceleration  $A_r(t)$  is calculated from the filtered acceleration components by the equation:
- $$A_r(t) = \sqrt{A_x(t)^2 + A_y(t)^2 + A_z(t)^2}.$$
- From this time series, local maximum points above a certain threshold are picked up. The time indices of these points are hereafter referred to as LMP. The threshold value is typically set to  $1.5 \text{ m/s}^2$  to ensure that other cyclic events with low intensity, such as tremor, can be excluded.
- Selection of a template wave is composed of  $p$  consecutive points centered at one of those LMP,  $[A_x(t_0) A_y(t_0) A_z(t_0)]$ . Typically,  $p$  is chosen as 50, which corresponds to a time interval of 0.5 sec when  $\Delta t = 10 \text{ msec}$ .
- Calculation of the normalized cross correlation between the template and all signal segments centered at other LMP,  $[A_x(t) A_y(t) A_z(t)]$  for  $0 \leq t - t_0 \leq 2 \text{ (sec)}$ .
- Among the segments with correlation coefficient  $> 0.5$ , a segment that yields the highest correlation coefficient is selected. The template wave is replaced with this segment wave. The existence of a segment with large correlation coefficient ( $> 0.5$ ) strongly suggests that the signal within the current time range is highly periodic.
- Procedures (3) and (4) are repeated until no segment waves with correlation coefficient  $> 0.5$  are found. The central time of the final template thus obtained is denoted as  $T_1$ .

- From the initial  $t_0$  and the template selected in procedure 2, procedures (3), (4), and (5) are repeated backward in time, that is,  $0 \leq t_0 - t \leq 2$ . The central time of the final template is denoted as  $T_2$ .
- The region between  $T_2$  and  $T_1$  is extracted from the acceleration signal. This is an active rhythm block characterized by highly rhythmic behavior of moderate or large intensity with a cycle duration of  $< 2$  sec.
- Procedures (2)–(7) are repeated. In this way, the entire time series is divided into active rhythm blocks and inactive and/or nonrhythmic blocks. The former can be regarded as continuously walking regions.

### 2.2.3. Estimation of stride peak candidates

From each of the continuously walking regions, stride peak candidates are estimated by the following template-matching algorithm:

- Selection of a point  $t_0$  from LMP and generation of a template wave with  $p$  consecutive points centered at this point. The template size  $p$  can be typically set to 50, but more precisely, it should be optimized based on the characteristic timescale of the original acceleration signal [42].
- Calculation of the normalized cross correlation between the template and all signal segments centered at other LMP.
- Selection of the segments with correlation coefficient  $> 0.5$ . Calculation of the average value of those correlation coefficients.
- Procedures (1)–(3) are repeated for all LMP. The template wave that yields the largest average correlation coefficient is chosen as the optimized template.
- Calculation of the normalized cross correlation time series by sliding the optimized template over the current continuously walking region.
- Extraction of the local maximum points from the normalized cross correlation time series. Among these points, the ones with positive correlation coefficient are the desired stride peak candidates.

Hereafter, the time index of the optimized template center is indicated by  $t_c$ .

### 2.2.4. Detection of stride peaks

The candidate peaks obtained so far are not fiducial points due to the possible presence of extra peaks related to the contact of both feet (step peaks) and other spurious points. Therefore, stride peaks are determined with the help of a “guide wave” by the following procedure:

- The three-dimensional acceleration signal  $[A_x(t) A_y(t) A_z(t)]$  is integrated twice in combination with high-pass filtering to avoid integration drift. The integrated signal  $[D_x(t) D_y(t) D_z(t)]$  corresponds to the relative displacement of the body where the device was attached.

This operation works to smooth the original signal and enhances the monophasic nature of medial/lateral movements during walking.

- (2) Consider a fixed unit vector pointing from  $[D_x(t_c - w) D_y(t_c - w) D_z(t_c - w)]$  to  $[D_x(t_c + w) D_y(t_c + w) D_z(t_c + w)]$  and an arbitrary unit vector pointing from  $[D_x(t - w) D_y(t - w) D_z(t - w)]$  to  $[D_x(t + w) D_y(t + w) D_z(t + w)]$  in 3D space. The inner product of these two vectors is calculated. The inner product is time-dependent, giving a new time series, which is called here “guide wave.” Here, the time range of the unit vector  $w$  is decided so that the obtained guide wave behaves like a square wave with the same monophasic pattern as the medial/lateral ( $x$ -axis) signal. Usually, it is almost equal to the time range of the optimized template wave, that is,  $2w = p$ .
- Selection of the candidate stride peak with the largest correlation coefficient per single guide wave cycle. These are fiducial stride peaks.

The method of making a guide wave is not limited to the one presented here. The key is to find a suitable monophasic signal, that is, a signal composed of a wavelet that is repeated once per single gait cycle. In [42], we designed a different type of guide wave by utilizing the anisotropic character of the  $x$ -axis acceleration signal.

**Figure 1B** and **C** illustrates the validity of this procedure. **Figure 1B** shows an example of the total acceleration wave. The center point of the optimized template is marked by an open circle. The detected peaks using the guide wave are indicated by asterisks in **Figure 1C**. It is clear that only the stride peaks, that is, gait peaks associated with the same leg, are selected, while peaks due to the other leg are not counted. In our earlier work, we found that this type of peak detection algorithm performs fairly well for the gait of PD patients under supervised but non-laboratory conditions, with more than 95% accuracy [43].

### 2.2.5. Estimation of “gait cycle duration” and “gait-induced acceleration”

After identifying correct stride peaks, the duration of a single gait cycle and the amplitude of gait-induced acceleration per cycle are calculated as follows. Let two adjacent stride peaks be indexed as  $i = 1$  and  $i = N$ . Then, the gait cycle duration is given by  $(N - 1)\Delta t$ , and gait acceleration is defined by  $\frac{\sum_{i=1}^{N-1} A_i(i\Delta t)}{N - 1}$ . These measures are calculated from all peak-to-peak intervals. Since gait accelerations correlate with floor reaction forces, the amplitude of gait acceleration is selected as an index of floor reaction force. Thus, the obtained gait cycle duration and the amplitude of gait-related acceleration are averaged for every 10-min period of recording.

### 2.2.6. Accuracy of analysis using pattern-matching method in detecting gait-induced signals

To further assess the sensitivity of the PGR, we compared the results of PGR with those of a standard system using floor reaction forces [unpublished data]. We asked the subject to step in response to a particular gait cycle determined by a metronome (0.87–1.30 sec) and compared the reappearance of the cycle recorded from the two devices.

Using the PGR, we recorded metronome-guided 10 m walking in six normal control subjects (age,  $43.3 \pm 7.7$  years, mean  $\pm$  SD, four men, and two women). The metronome was set at 92, 100, 112,



120, 132, and 138 beats per minute. The subjects were asked to contact the right or left foot corresponding to the beat. Thus, the expected gait cycle (the duration from the ground contact of one foot to the next contact of the same foot) was 1.30, 1.20, 1.07, 1.00, 0.91, and 0.87 sec, respectively.

In this control study, subjects equipped with the PGR device walked on the force plate (WalkWay MW-1000, Anima, Tokyo). Since the force plate was 2.4 m long, only part of the metronome-guided 10 m walking was recorded simultaneously by the two devices. The gait cycles recorded by the two equipments were compared across all subjects and all metronomic paces by using the Bland–Altman plot and intraclass correlation (ICC (2,1)) methods. The subjects were asked to walk in sync with the beats of the metronome. The cycle of the metronome-guided walking was set at five stages: 1.30, 1.20, 1.07, 1.00, 0.91, and 0.87 sec. **Figure 3** shows an example of the recorded accelerations by PGR during the metronome recording. **Figure 3A** shows an example where a difference was observed between the expected and recorded gait cycles. The expected cycle was 0.87 sec, whereas the recorded cycle was 0.94 sec. On the other hand, **Figure 3B** shows an example where the recorded gait cycle matched the expected gait cycle.

**Table 2** shows a summary of the gait cycles recorded by the PGR and the force plate, for each subject. We could not identify the gait cycle from the force plate data in four cases out of the total of 36 measurements. Therefore, we used 32 pairs of data for comparison of the two methods. **Figure 3C** shows the Bland–Altman plot, demonstrating the difference in two gait cycles as a function of their mean values. The 95% confidence interval of the mean difference was  $[-0.0191$  to  $0.0003]$ , which includes zero, and no significant regression was observed ( $p = 0.49$ ),

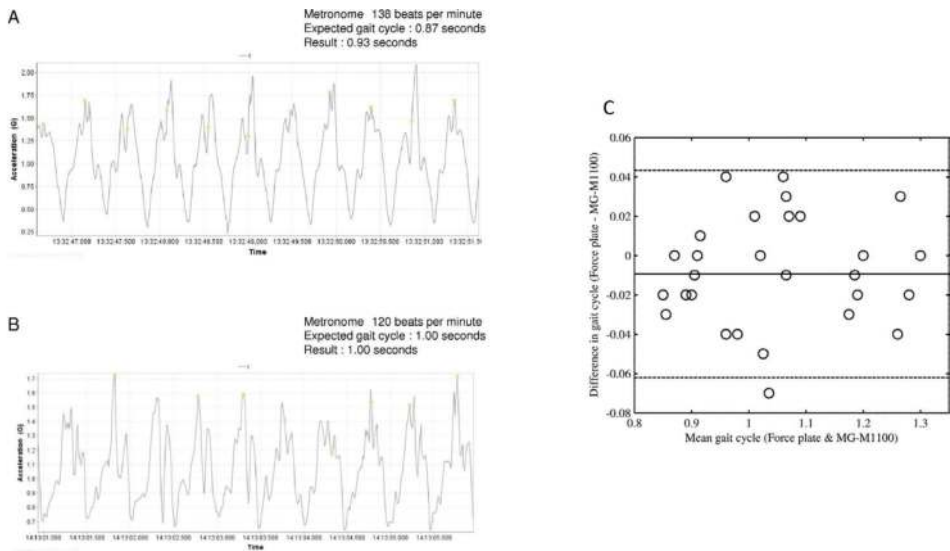


**Figure 3.** (A, B) Examples of gait-induced accelerations during metronome-guided walking. The expected rate defined by the metronome was 0.87 sec in (A) and 1.00 sec in (B). (C) Bland–Altman plot of two gait cycles estimated by force plate and PGR. The differences between the two sets of gait cycles are plotted against their mean values. The solid line represents the mean difference, while the dashed lines are the 95% confidence limit lines (bias  $\pm$  1.96 SD).

Metronome (beats/min)	92	100	112	120	132	138
Expected gait cycle (sec)	1.30	1.20	1.07	1.00	0.91	0.87
Subject 1						
Force plate (sec)		1.10	1.08	1.08		0.98
MG-M1100 (sec)	1.18	1.08	1.05	1.04	1.01	0.94
Subject 2						
Force plate (sec)	1.27	1.18	1.00	0.94	0.88	0.84
MG-M1100 (sec)	1.29	1.19	1.05	0.98	0.90	0.86
Subject 3						
Force plate (sec)	1.24	1.18	1.06	1.02	0.92	
MG-M1100 (sec)	1.28	1.20	1.07	1.00	0.91	0.87
Subject 4						
Force plate (sec)	1.30	1.20	1.06	0.96	0.89	0.87
MG-M1100 (sec)	1.30	1.20	1.07	1.00	0.91	0.87
Subject 5						
Force plate (sec)	1.28	1.16	1.00	0.96	0.91	0.84
MG-M1100 (sec)	1.25	1.19	1.07	1.00	0.91	0.87
Subject 6						
Force plate (sec)		1.20	1.08	1.02	0.90	0.84
MG-M1100 (sec)	1.26	1.20	1.06	1.02	0.91	0.87

**Table 2.** Recorded gait cycle during metronome-guided walking.

suggesting that there was no systematic error in the Bland-Altman plot. Moreover, the two gait cycles yielded a fairly high ICC value of 0.98 ( $p < 0.0001$ ), with 95% confidence interval value of [0.96-0.99]. These results indicate that the recorded gait cycle by the PGR was statistically in good agreement with that of the force plate. The results showed no significant differences between the two methods, indicating that PGR accurately monitors gait movements with sensitivity comparable to that of the force plates. Since more steps were analyzed in the recordings using PGR than those using the force plate, fluctuation appears to be small. The results of the control experiments indicate that PGR can quantitatively estimate gait disorders in daily life with good sensitivity.

### 2.2.7. Merits of proposed gait measures

One notable merit of the developed method is that both gait cycle duration and gait-induced acceleration can serve as quantitative indices for the assessment of daily gait performance. Other basic parameters that are widely used in gait analysis are walking speed and step length. While these two parameters are not measured directly by our method, it is possible to estimate them with good accuracy from the recorded gait measures, since there is a close

correlation between (logarithm of) gait-induced acceleration and walking speed, when these two parameters are expressed by body height [50].

However, it should be noted that any gait parameter, when used separately, is more than often insufficient to allow complete understanding of ambulatory gait behavior. For example, a person usually changes gait cycle duration (or cadence) over the course of a day both voluntarily and involuntarily. Real life comprises a diversity of environmental constraints, making it almost impossible for us to keep on walking freely. Therefore, even if the gait parameter appears to deteriorate in a certain time of the day, one cannot decide whether it is caused by disorders in internal factors (e.g., the subject's physical conditions) or by changes in walking pace due to external perturbations. In most cases, such "forced" changes are transient, and their effects could be reduced by taking the long-time average of the parameter. However, the combination of gait cycle duration and gait acceleration provides a more powerful solution to this problem, as will be demonstrated in this paper and as was reported previously [43, 44]. The two measures, when plotted on a plane, will fall on a rather well-ordered structure that is individual-specific and robust against external constraints. The robustness of the gait cycle-acceleration relationship is considered to result from the human tendency to automatically select preprogrammed preferred walking behavior in response to environmental changes [43]. Based on this property, we can obtain insightful information on intrinsic gait problems from ambulatory monitoring, which is the greatest merit of using the proposed gait measures.

### 3. Quantification of "poverty of movements" and "slowness/smallness in executed movements": "amount of overall movements per 24 hrs"

Poverty in movements and slowness/smallness in executed movements are the core motor clinical signs of PD. Overall activities should be examined to quantify these two clinical signs. In order to quantify overall activities, we analyzed the distribution of 10-min averaged various movement-induced accelerations (**Figure 4A** and **B**) and calculated the mean value of the distribution with the assumption that the curve fits with gamma distribution [45, 53]. The gamma distribution is defined by the following formula:

$$f(x) = x^{k-1} e^{-x/\theta} / \Gamma(k) \theta^k \text{ for } x > 0$$

The mean value was defined as the *amount of overall movements per 24 hrs*, representing an index of poverty of movements and slowness/smallness of executed movements.

A total of 50 patients with PD and 17 normal control subjects participated in this analysis [45]. The distribution curve shifted to the left, suggesting a decrease in activities (**Figure 4A** and **B**). The *amount of overall movements per 24 hrs* was smaller in PD patients compared with the mean value of normal control subjects ( $0.69 \pm 0.19$  m/sec<sup>2</sup>). Furthermore, 38 of the 50 patients (76%) showed a decrease below 0.50 m/sec<sup>2</sup>, the value of mean (1sd). The *amount of overall movements per 24 hrs* decreased in proportion with the severity of PD. The *amount of overall movements per 24 hrs* for patients with score  $\geq 30$  ( $0.31 \pm 0.09$  m/sec<sup>2</sup>) was significantly lower than that of

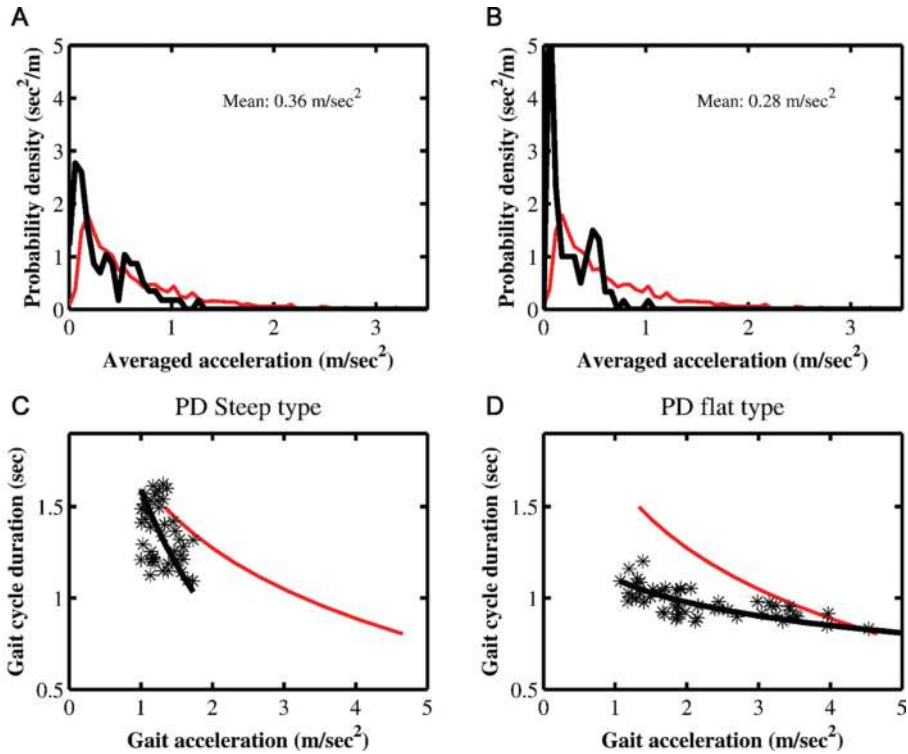


**Figure 4.** (A, B) Probability distribution of the averaged acceleration per 10 min, obtained from 24 hrs of continuous recording. (C, D) examples of gait acceleration-cycle duration relationship in a patient with Parkinson's disease (PD) based on 24 hrs of gait recording. Black thick line: Corresponding regression line. In (C) and (D), red thin line: Regression line obtained from the summed average of 17 normal control subjects. The regression line of the PD patient is steep in (C), whereas it is flat in (D).

patients with scores 1–15 ( $0.40 \pm 0.09 \text{ m/sec}^2$ ) ( $p < 0.05$ ) and that of patients with scores 16–30 ( $0.48 \pm 0.09 \text{ m/sec}^2$ ) ( $p < 0.01$ ). Furthermore, in 50 patients with untreated PD, the *amount of overall movements per 24 hrs* was significantly associated with the UPDS part II score and part III score [53]. These results suggest that the *amount of overall movements per 24 hrs* can be a good index for poverty of movements and slowness/smallness of executed movements in ADL.

## 4. Quantitative estimation of parkinsonian gait using two parameters: “gait-induced acceleration” and “gait cycle duration”

### 4.1. Relationship between gait-induced acceleration and gait cycle duration

The relationship between gait-induced acceleration and gait cycle duration (*gait acceleration-cycle duration curves*) [45, 46] is shown in **Figure 4C** and **D**. Both parameters were recorded continuously for more than 24 hrs, and then the average value of every 10 min was computed

and plotted. Interestingly, a regression line can be determined for the plotted data. In **Figure 4C** and **D**, the thick black line represents the regression line of data of a PD patient, while the thin red line represents the regression line for the data of 17 normal control subjects. The data clearly show a correlation between accelerations and cycle; for example, walking with a slow cycle is associated with low amplitude of gait accelerations. The slope of the linear regression line for data of the normal control subjects was  $1.20 \pm 0.29$ .

The *gait acceleration-cycle duration curves* of PD patients showed two distinct patterns compared to those of normal control subjects [45, 46]. First, the position of the curve in PD deviated from that of the normal control curve; the curve of PD patients was shifted to the left on the acceleration axis (**Figure 4C** and **D**), suggesting a decrease in the mean amplitude of gait-induced acceleration. Furthermore, the curve of PD patients was shifted upward (**Figure 4C**) or downward (**Figure 4D**) on the gait cycle duration axis, suggesting prolongation or shortening of the mean gait cycle duration, respectively. Second, the range value around the regression line was narrow in PD patients [45, 46]. A narrow range of acceleration was associated with a steep slope of the regression line (**Figure 4C**), whereas a narrow range of gait cycle duration was associated with a flat slope of the regression line (**Figure 4D**).

Based on these findings, we next quantified these two kinds of changes in the *gait acceleration-cycle duration curve*, that is, changes in the mean value and range, as described below.

#### **4.2. Changes in mean values of gait-induced acceleration and gait cycle duration: Possible index of PD deficits in gait control neural circuits**

We first examined changes in the mean amplitude of gait-induced acceleration and gait cycle duration during daily walking in 64 PD patients and 17 normal control subjects [48]. The mean values of the gait-induced acceleration and gait cycle duration were computed (**Figure 5**). PD patients walked with significantly lower gait accelerations compared with normal control subjects, but there were no significant differences among the disease stage groups. In contrast, PD patients with modified Hoehn and Yahr (mH&Y) stage 1.5 walked with significantly faster gait cycle duration (faster rhythm) than those with stages 2.5–3.0 and normal control subjects, although there was no significant difference in gait cycle duration between patients with stages 2.5–3.0 PD and normal control subjects. The lower gait accelerations (i.e., inappropriate force production) can be the cause of narrow stride [42, 43]. Thus, the above results suggest that PD patients cannot walk with a sufficient stride throughout the clinical course, which can be compensated by increasing stepping [48, 55–57] at the early stage, but not at the advanced stage [48]. Our data suggest that computation of acceleration of gait movements and gait cycle duration from daily walking can be useful in the assessment of the clinical stage of the gait disorder.

#### **4.3. Narrow range of gait-induced acceleration and gait cycle duration: Possible index of monotony in PD**

Another characteristic change in the shape of the *gait acceleration-cycle duration curve* is the narrowness of the range of force and/or rhythm [45, 46]. When PD patients walked with a narrow range of change in gait acceleration (i.e., floor reaction forces), the slope of the regression line was steep (*steep type*) (**Figure 4C**). In contrast, when PD patients walked with a narrow

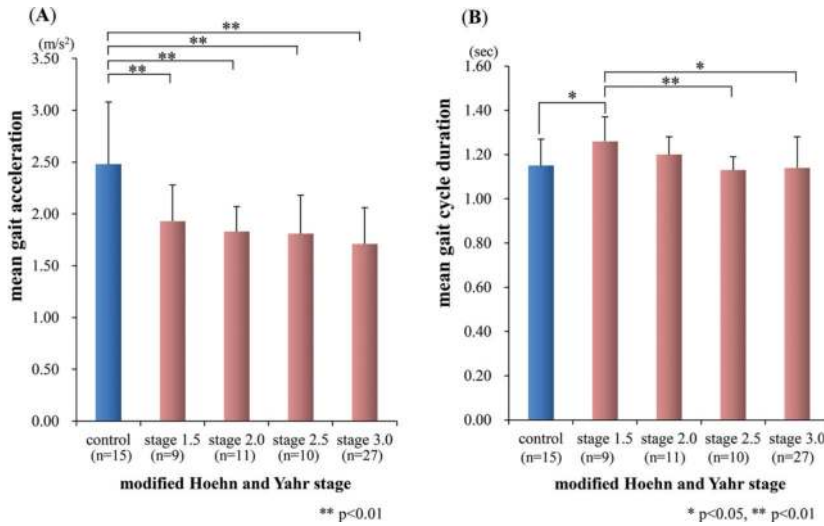


**Figure 5.** The mean gait acceleration (A) and mean gait cycle (B) in PD patients according to the modified Hoehn and Yahr stages. Differences between each stage group and normal control subjects, and among the stage groups were analyzed for statistical significance ( $*p < 0.05$ ,  $**p < 0.01$ , by *t*-test) [40].

range of change in the gait cycle duration (i.e., rhythm), the regression line was flat (*flat type*) (Figure 4D). Other patients walked with a narrow range of both acceleration and cycle, and their acceleration and cycle duration data were scattered within a narrow range (*lump type*). Under these conditions, the patient always walks with the preferred floor reaction forces or cycle, that is, monotone walking.

For quantitative assessment of these changes, we defined *%alteration range* as an index of monotone walking [46]. The mean and standard deviation (SD) of gait acceleration and cycle duration were calculated from the *gait acceleration-step cycle duration curve*, which was constructed from a single long-term recording from each patient. Here, we used the SD as an index of alteration range. The interindividual mean of SD was calculated from data of 17 control subjects. Thus, the ratio of the SD of each patient to the interindividual mean of SD of the normal control subjects was defined as *%alteration range*. The cutoff level was set at 75% in analysis of the *%alteration range*.

Changes in *%alteration range* were examined in 40 patients with PD. In this analysis, the regression in 16 of the 40 (40%) patients was similar to that of the control (*%alteration range* > 75%). Furthermore, the *steep type* (*%alteration range* of gait acceleration of <75%) was identified in 12 of the 40 patients (30%), whereas the *flat type* (*%alteration range* of gait cycle of <75%) was noted in 8 of the 20 (20%) patients, and the *lump pattern* was noted in 10% of patients (4/40) [46].

It has been reported that the maximum activities that can be generated in a muscle burst is low in PD patients [58] and that PD patients can only execute movements of different amplitudes at a single, slow velocity without dynamic changes of the movement velocity [59]. These studies suggest a possible mechanism for the narrow range of force and rhythm in gait, that

is, PD patients cannot dynamically vary the force and rhythm in their daily walking, resulting in a narrow range of floor reaction forces and step cycles. Our data suggest that quantification of both the range of gait-induced acceleration and gait cycle duration provides a useful index of monotony, a fundamental pathophysiology in PD.

## 5. Quantitative estimation of motor fluctuation

Although dopamine replacement therapy is effective at the early stage, patients with PD develop motor fluctuation as the disease progresses [13, 47, 60–62]. By detecting changes in gait parameters, we tried to determine motor fluctuations. We review here the following two methods.

### 5.1. Method I: identification of “off” by tracing daily changes in gait-induced accelerations and gait cycle duration

We traced changes in gait-induced accelerations and cadences (steps/min, a parameter identical to gait cycle duration). These changes in gait force and rhythm parameters were compared simultaneously with patients’ diaries. A total of 44 patients with PD, who showed simultaneous changes between accelerations and cadences, and 17 normal control subjects participated in this study [47].

No subjective fluctuations were noticed by 23 of these 44 patients. However, the PGR detected pathological shift of accelerations and cadences in 19 of the 23 patients (83%). These patients showed fast stepping or slow stepping with low amplitude of accelerations. On the other hand, the other 21 patients complained of subjective off in their diaries. Long-term tracing of gait-induced accelerations and cadences identified no changes in 11 of these 21 patients (52%). Surprisingly, no synchronization was noted between the subjective off and gait off determined by the PGR in 30 of the 44 patients (68%). This discrepancy could be in part due to deficits in attention to motor deficits [63]. Our data suggest that tracing simultaneous changes in acceleration and cadence can raise an interesting question: “How do PD patients subjectively notice the off time?”

Clinically, improvements in gait fluctuations of PD patients after the addition or increase in dose of an anti-parkinsonism medicine were detected by examining changes in gait force and rhythm parameters [54]. The present method had a high sensitivity for detecting improvements than the UPDRS scores.

### 5.2. Method II: quantitation of degree of motor fluctuation by calculating frequency mode change in gait

#### 5.2.1. Two strategies

We reported previously [42, 43] that the relationship between gait-induced acceleration and gait cycle duration can be described by the following function derived from an inverted pendulum model:

$$a_v = \frac{1}{T_c} \left[ \alpha \left( \frac{1}{T_c} - \frac{1}{T_0} \right) + \beta \right]^2,$$

where  $T_c$  is the gait cycle,  $a_v$  is the vertical acceleration magnitude averaged over  $T_c$ , and  $\alpha$ ,  $\beta$ , and  $T_0$  are the three separate parameters. Parameters  $\alpha$  and  $\beta$  are subject-specific, representing a particular walking strategy of an individual,  $\alpha$  quantifies how to regulate gait acceleration according to different gait paces, and  $\beta$  is something like a basic potential force that drives natural walking. In contrast,  $T_0$  is assumed to be a constant across subjects. Specifically, we set  $T_0 = 1.4$  sec in order to uncorrelate  $\alpha$  and  $\beta$  with each other [42, 43]. The above mathematical method was used to build better fitting regression curves from the data. In other words, this mathematical method for regression curves represents improvement compared to that shown in Figure 4C and D.

Figure 6A shows that two regression lines are necessary for better fitting of plots obtained from long-term daily walking, suggesting that a subject usually walks with two types of gait mode [49]. The steep regression line with small accelerations for a particular cycle means quiet walking, for example, walking within the house, whereas the flat regression line with large accelerations for a particular cycle reflects active walking, for example, walking in the street. These results suggest that the subject changes the walking strategy during daily walking between “quiet mode” and “active mode.” To identify the involvement of deficits in higher functions, we quantitatively examined the “switching” from one mode to another [49].

### 5.2.2. Frequency of mode change

A total of 26 patients with PD and 13 normal control subjects participated in this study [49]. We introduced the parameter of *frequency of mode change* (FC), which describes the frequency of changes in walking strategies and is calculated mathematically by the following equation:

$$FC = \frac{\sum_{t=1}^{n-1} |I(t+1) - I(t)|}{n-1},$$

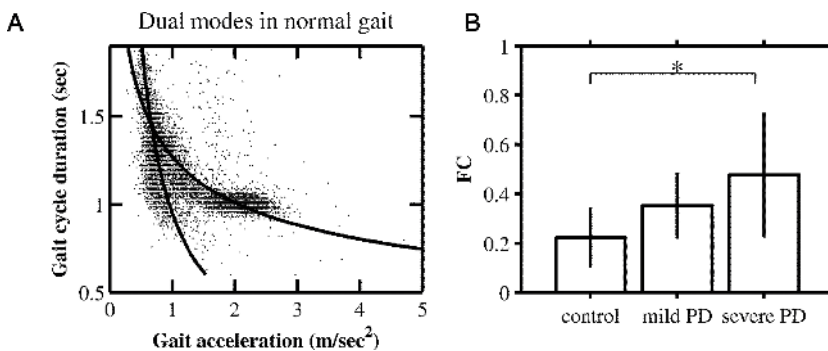


Figure 6. (A) Examples of gait acceleration-cycle duration relationship in a normal subject based on 24 hrs of gait recording. The amplitude of gait-related accelerations and duration of gait cycles were plotted for all stride events. Two regression lines were required for better fitting. (B) Frequency of mode change (FC) that describes the frequency of changes into different walking strategies between quiet mode and active mode.



where  $I(t)$  reflects the walking mode [i.e., active (0) or quiet (1)] in each non-overlapping 1 hr. interval during the day and  $t$  signifies the time index [ $t = 1, 2, \dots, n$  ( $n \leq 24$ )]. FC was  $0.22 \pm 0.12$  in normal subjects compared with  $0.35 \pm 0.13$  in patients with mild PD (mH&Y stage  $< 2.5$ ) and  $0.48 \pm 0.25$  in patients with severe PD (mH&Y stage  $\geq 2.5$ ) ( $p < 0.05$ ) (**Figure 6B**) [49]. In PD, the quiet mode coincides approximately with slow stepping gait mode. These results show that estimation of frequency of change between quiet and active modes provides an estimate of the degree of motor fluctuation.

## 6. Conclusion

Our newly developed wearable device and algorithm, the PGR, allows continuous monitoring of gait for up to 70 hrs and can differentiate precisely gait-induced accelerations from other movements. The PGR can monitor both the overall motor activities and gait movements in daily activities. The findings obtained from long-term monitoring using PGR are classified into three categories.

### 6.1. Poverty of movements and slowness/smallness of executed movements

Acceleration values induced by various movements, averaged every 10 min, showed gamma distribution. The mean value in this distribution was used as an index of the *amount of overall movements per 24 hrs*. The *amount of overall movements per 24 hrs* was lower in PD patients, especially in patients with UPDRS-III  $\geq 30$ , suggesting that this parameter reflects the range from poverty of movements to slowness/smallness of executed movements.

### 6.2. Gait disorders

Analysis of the *gait acceleration-cycle duration curve* provided the mean values and ranges of gait-induced acceleration and gait cycle duration. Quantitative analysis showed force generation deficits, disabilities of gait rhythm setting, and loss of dynamic modulation of the force and rhythm in each patient with PD. The quantitative measures can be used for assessment of the degree of parkinsonian gait disorders. These changes in gait-induced acceleration reflect PD-specific deficits in neural circuits involved in gait control [1, 2, 10]. Thus, it is hoped that long-term monitoring of these parameters can identify the pathophysiological changes in gait disorders in PD.

### 6.3. Motor fluctuation

Furthermore, the device also provides assessment of motor fluctuation from the data of gait fluctuation in any particular day. By tracing changes in gait-induced accelerations and gait cycle durations, we identified the time of motor off, which was not necessarily noticed by patients. Measurement of the frequency of changes in quiet mode (i.e., slow stepping mode) and active mode provides information on the degree of severity of motor fluctuation.

### 6.4. Open questions and possible clinical applications

Taken together, measurement of overall movement- and gait-induced accelerations using a wearable device could be useful for clinical assessment of parkinsonian status. Especially, the

---

Quantification of “poverty of movements” and “slowness/ smallness of executed movements”:

- Acceleration values induced by various movements are averaged every 10 min from the long-term monitoring data
- The mean value in this gamma distribution can be an index of the *amount of overall movements per 24 hrs*

Gait disorders:

- Gait-induced accelerations are averaged every 10 min from the long-term monitoring data
- The *gait acceleration-cycle duration curve* is calculated from these plots
- Changes in the mean values of acceleration and cycle duration can reflect deficits in force production and rhythm setting mechanisms, respectively
- Narrowness of accelerations and cycle duration can reflect loss of dynamic modulation of the force and rhythm control

Motor fluctuation:

- The time of motor off can be determined by tracing changes in gait-induced accelerations and gait cycle durations
  - Measurement of frequency of changes between quiet and active modes provides an index of the severity of motor fluctuation
- 

**Table 3.** Protocol for quantitative assessment of poverty of movements and slowness/smallness of executed movements, gait disorders, and motor fluctuation.

new algorithm that defines the relationship between gait-induced acceleration and gait cycle duration could be useful in clinical applications. However, there are still the following open questions:

- Our studies were conducted in a small number of normal subjects and patients with PD. Thus, the outcome from our data has not been validated.
- Methodologically, our analysis does not include quantification of stride length. For example, analysis using an inverted pendulum model should be useful [64].

Here, we provisionally propose a comprehensive and quantitative examination protocol for poverty of movements and slowness/smallness of executed movements, gait disorders, and motor fluctuation in patients with PD using an accelerator-mounted wearable device (see **Table 3**). This physiology-based protocol would make it possible to quantify the extent of parkinsonian motor signs and/or the effect of drugs. We anticipate that further analysis of daily walking using the PGR would contribute to the development of better therapies for PD.

## Conflict of interest

The authors declare no conflict of interest.

## Author details

Masahiko Suzuki<sup>1\*</sup>, Makiko Yogo<sup>1</sup>, Masayo Morita<sup>1</sup>, Hiroo Terashi<sup>2</sup>, Mutsumi Iijima<sup>3</sup>, Mitsuru Yoneyama<sup>4</sup>, Masato Takada<sup>5</sup>, Hiroya Utsumi<sup>6</sup>, Yasuyuki Okuma<sup>7</sup>, Akito Hayashi<sup>8</sup>, Satoshi Orimo<sup>9</sup> and Hiroshi Mitoma<sup>10</sup>

\*Address all correspondence to: [suzukimd@jikei.ac.jp](mailto:suzukimd@jikei.ac.jp)

1 Department of Neurology, Katsushika Medical Center, The Jikei University School of Medicine, Tokyo, Japan

2 Department of Neurology, Tokyo Medical University, Tokyo, Japan

3 Department of Neurology, Tokyo Women's Medical University, Tokyo, Japan

4 Mitsubishi Chemical Corporation, Yokohama R&D Center, Yokohama, Japan

5 LSI Medience Corporation, Tokyo, Japan

6 Department of Neurology, Shioya Hospital, International University of Health and Welfare, Tochigi, Japan

7 Department of Neurology, Shizuoka Hospital, Juntendo University, Shizuoka, Japan

8 Department of Rehabilitation, Urayasu Hospital, Juntendo University, Chiba, Japan

9 Department of Neurology, Kanto Chuo Hospital, Tokyo, Japan

10 Medical Education Promotion Center, Tokyo Medical University, Tokyo, Japan

## References

- [1] Dietz V. Human neuronal control of automatic functional movements: Interaction between central programs and afferent input. *Physiological Reviews*. 1992 Jan;**72**(1):33-69
- [2] Dietz V. Neurophysiology of gait disorders: Present and future application. *Electroencephalography and Clinical Neurophysiology*. 1997 Sep;**103**(3):333-355
- [3] Schaafsma JD, Balash Y, Gurevich T, Bartels AL, Hausdorff JM, Giladi N. Characterization of freezing of gait subtypes and the response of each to levodopa in Parkinson's disease. *European Journal of Neurology*. 2003 Jul;**10**(4):391-398
- [4] Critchley M. Arteriosclerotic parkinsonism. *Brain*. 1929;**52**:23-83
- [5] Nutt JG, Marsden CD, Thompson PD. Human walking and higher-level gait disorders, particularly in the elderly. *Neurology*. 1993 Feb;**43**(2):268-279
- [6] Thompson PD, Marsden CD. Gait disorder of subcortical arteriosclerotic encephalopathy: Binswanger's disease. *Movement Disorders*. 1987;**2**(1):1-8

- [7] Thompson PD. Gait Disorders Accompanying Diseases of the Frontal Lobes. In: Růžička E, Hallet M, Jankovic J, editors. *Advances in Neurology. Gait Disorders*. Philadelphia, USA: Lippincott Williams & Wilkins; 2001. pp. 235-241
- [8] Nutt JG. Gait disorders. In: Jankovic J, Tolosa E, editors. *Parkinson's disease and movement disorders*. Baltimore, USA: Urban & Schwarzenberg; 1988. pp. 377-383
- [9] FitzGerald PM, Jankovic J. Lower body parkinsonism: Evidence for vascular etiology. *Movement Disorders*. 1989;4(3):249-260
- [10] Mitoma H, Hayashi R, Yanagisawa N, Tsukagoshi H. Characteristics of parkinsonian and ataxic gaits: A study using surface electromyograms, angular displacements and floor reaction forces. *Journal of the Neurological Sciences*. 2000 Mar;174(1):22-39
- [11] Fahn S, Elton RL. UPDRS Development Committee. Unified Parkinson's Disease Rating Scale. In: Fahn S, Marsden CD, Calne D, Goldstein M, editors. *Recent Development in Parkinson's Disease*. Florham Park, NJ: Macmillan; 1987. pp.153-164
- [12] Weiss A, Mirelman A, Buchman AS, Bennet DA, Hausdorff JM. Using a body-fixed sensor to identify subclinical gait difficulties in older adults with IADL disability: Maximizing the output of the time up and go. *PLoS One*. 2013 Jul 29;8(7):e6885
- [13] Knutsson E. An analysis of parkinsonian gait. *Brain*. 1972;95:475-486
- [14] Maetzler W, Domingos J, Srulijes K, Ferreira JJ, Bloem BR. Quantitative wearable sensors for objective assessment of Parkinson's disease. *Movement Disorders*. 2013 Oct;28(12):1628-1637
- [15] Kubota KJ, Chen JA, Little MA. Machine learning for large-scale wearable sensor data in Parkinson's disease: Concepts, promises, pitfalls, and futures. *Movement Disorders*. 2016 Sep;31(9):1314-1326
- [16] Hobert MA, Maetzler W, Aminian K, Chiari L. Technical and clinical view on ambulatory assessment in Parkinson's disease. *Acta Neurologica Scandinavia*. 2014 Sep; 130(3):139-147
- [17] Pasluosta CF, Gassner H, Winkler J, Klucken J, Eskofier BM. An emerging era in the management of Parkinson's disease: Wearable technologies and the internet of things. *IEEE Journal of Biomedical and Health Informatics*. 2015 Nov;19(6):1873-1881
- [18] Godinho C, Domingos J, Cunha G, Santos AT, Fernandes RM, Abreu D, Gonçalves N, Matthews H, Isaacs T, Duffen J, Al-Jawad A, Larsen F, Serrano A, Weber P, Thoms A, Sollinger S, Graessner H, Maetzler W, Ferreira JJ. A systematic review of the characteristics and validity of monitoring technologies to assess Parkinson's disease. *Journal of NeuroEngineering and Rehabilitation*. 2016;13:24
- [19] Dijkstra B, Kamsma YP, Zijlstra W. Detection of gait and postures using a miniaturized triaxial accelerometer-based system: Accuracy in patients with mild to moderate Parkinson's disease. *Archives of Physical Medicine and Rehabilitation*. 2010;91(8):1272-1277

- [20] de Groot S, Nieuwenhuizen MG. Validity and reliability of measuring activities, movement intensity and energy expenditure with the DynaPort MoveMonitor. *Medical Engineering & Physics*. 2013;**35**(10):1499-1505
- [21] Mancini M, Horak FB. Potential of APDM mobility lab for the monitoring of the progression of Parkinson's disease. *Expert Review of Medical Devices*. 2016;**13**(5):452-466
- [22] Dewey DC, Miocinovic S, Bernstein I, Khemani P, Dewey RB III, Query R, Chitnis S, Dewey RB Jr. Automated gait and balance parameters diagnose and correlate with severity in Parkinson disease. *Journal of the Neurological Sciences*. 2014;**345**(1-2):131-138
- [23] Mariani B, Jiménez MC, Vingerhoets FJG, Aminian K. On-shoe wearable sensors for gait and turning assessment of patients with Parkinson's disease. *IEEE Transactions on Biomedical Engineering*. 2013;**60**(1):155-158
- [24] Fisher JM, Hammerla NY, Ploetz T, Andras P, Rochester L, Walker RW. Unsupervised home monitoring of Parkinson's disease motor symptoms using body-worn accelerometers. *Parkinsonism and related disorders*. 2016. DOI: [doi.org/10.1016/j.parkreldis.2016.09.009](https://doi.org/10.1016/j.parkreldis.2016.09.009)
- [25] Suzuki M, Mitoma H, Yoneyama M. Quantitative analysis of motor status in Parkinson's disease using wearable devices. From methodological considerations to problems in clinical applications. *Parkinson's Disease*. 2017. Article ID 6139716
- [26] van Hilten JJ, Middelkoop HA, Kerkhof GA, Roos RA. A new approach in the assessment of motor activity in Parkinson's disease. *Journal of Neurology, Neurosurgery, and Psychiatry*. 1991 Nov;**54**(11):976-979
- [27] Saito N, Yamamoto T, Sugiura Y, Shimizu S, Shimizu M. Lifecorder: A new device for the long-term monitoring of motor activities for Parkinson's disease. *Internal Medicine*. 2004 Aug;**43**(8):685-692
- [28] Hoff JI, van den Plas AA, Wagemans EA, van Hilten JJ. Accelerometric assessment of levodopa-induced dyskinesias in Parkinson's disease. *Movement Disorders* 2001 Jan;**16**(1):58-61
- [29] Hoff JI, van den Meer V, van Hilten JJ. Accuracy of objective ambulatory accelerometry in detecting motor complications in patients with Parkinson's disease. *Clinical Neuropharmacology* 2004 Mar-Apr;**27**(2):53-57
- [30] Steins D, Sheret I, Dawes H, Esser P, Collett J. A smart device inertial-sensing method for gait analysis. *Journal of Biomechanics*. 2014 Nov 28;**47**(15):3780-3785
- [31] Cancela J, Pastorino M, Arredondo MT, Nikita KS, Villagra F, Pastor MA. Feasibility study of a wearable system based on a wireless body area network for gait assessment in Parkinson's disease patients. *Sensors (Basel, Switzerland)*. 2014 Mar;**14**(3):4618-4633
- [32] Godfrey A, Del Din S, Barry G, Mathers JC, Rochester L. Instrumenting gait with an accelerometer: a system and algorithm examination. *Medical Engineering & Physics*. 2015 Apr;**37**(4):400-407

- [33] Rispens SM, van Schooten KS, Pijnappels M, Daffertshofer A, Beek PJ, van Dieen JH. Identification of fall risk predictors in daily life measurements: Gait characteristics' reliability and association with self-reported fall history. *Neurorehabilitation and Neural Repair*, 2015 Jan; **29**(1):54-61
- [34] van Schooten KS, Pijnappels M, Rispens SM, Elders PJ, Lips P, van Dieen JH. Ambulatory fall-risk assessment: Amount and quality of daily-life gait predict falls in in daily life measurements: Gait characteristics' reliability and association with self-reported fall history. *Neurorehabilitation and Neural Repair*. 2015 Jan;**29**(1):54-61
- [35] Del Din S, Hickey A, Hurwitz N, Mathers JC, Rochester L, Godfrey A. Measuring gait with an accelerometer-based wearable: Influence of device location, testing protocol and age. *Physiological Measurement*. 2016 Sep 21;**37**(10):1785-1797
- [36] Del Din S, Godfrey A, Mazzà C, Lord S, Rochester L. Monitoring of Parkinson's disease: Lesson from the field. *Movement Disorders*. 2016 Sep;**31**(9):1293-1313
- [37] Weiss A, Brozgol M, Dorfman M, Herman T, Shema S, Giladi N, Hausdorff JM. Does the evaluation of gait quality daily life provide insight into fall risk ? A novel approach using 3-day accelerometer recordings. *Neurorehabilitation and Neural Repair*. 2013 Oct;**27**(8):742-752
- [38] Weiss A, Herman T, Giladi N, Hausdorff JM. Objective assessment of fall risk in Parkinson's disease using a body-fixed sensory worn for 3 days. *PLoS One*. 2014 May 6;**9**(5): e96675
- [39] Weiss A, Herman T, Giladi N, Hausdorff JM. New evidence for gait abnormalities among Parkinson's disease patients who suffer from freezing of gait: Insights using a body-fixed sensor worn for 3 days. *Journal of Neural. Transmission (Vienna)*. 2015 Mar;**122**(3):403-410
- [40] Weiss A, Brozgol M, Giladi N, Hausdorff JM. Can a single lower trunk body-fixed sensor differentiate between level-walking and stair descent and ascent in older adults? Preliminary findings. *Medical Engineering & Physics*. 2016 Oct;**38**(10):1146-1151
- [41] Mitoma H, Yoneyama M, Orimo S. 24-hour recording of parkinsonian gait using a portable gait rhythmogram. *Internal Medicine*. 2010;**49**(22):2401-2408
- [42] Yoneyama M, Mitoma H, Watanabe K, Kurihara Y. Accelerometry-based gait analysis and its application to Parkinson's disease assessment. Part 1: Detection of stride event. *IEEE Transactions on Neural Systems and Rehabilitation Engineering*. 2014 May;**22**(3):613-622
- [43] Yoneyama M, Mitoma H, Watanabe K, Kurihara Y. Accelerometry-based gait analysis and its application to Parkinson's disease assessment. Part 2: A new measure for quantifying walking behavior. *IEEE Transactions on Neural Systems and Rehabilitation Engineering*. 2013 Nov;**21**(6):999-1005
- [44] Yoneyama M, Mitoma H, Okuma Y. Accelerometry-based long-term monitoring of movement disorders: From diurnal gait behavior to nocturnal bed mobility. *Journal of Mechanics in Medicine and Biology*. 2013;**13**:1350041

- [45] Utsumi H, Terashi H, Ishimura Y, Takazawa T, Hayashi A, Mochizuki H, Okuma Y, Orimo S, Takahashi K, Yoneyama M, Mitoma H. Quantitative assessment of gait bradykinesia in Parkinson's disease using a portable gait rhythmogram. *Acta Medica Okayama*. 2012;**66**(1):31-40
- [46] Terashi H, Utsumi H, Ishimura Y, Takazawa T, Okuma Y, Yoneyama M, Mitoma H. Deficits in scaling of gait force and cycle in parkinsonian gait identified by long-term monitoring of acceleration with the portable gait rhythmogram. *ISRN Neurology*. 2012:e306816
- [47] Utsumi H, Terashi H, Ishimura Y, Takazawa T, Okuma Y, Yoneyama M, Mitoma H. How far do the complaints of patients with Parkinson's disease reflect motor fluctuation? Quantitative analysis using a portable gait rhythmogram. *ISRN Neurology*. 2012:e372030
- [48] Terashi H, Utsumi H, Ishimura Y, Mitoma H. Independent regulation of the cycle and acceleration in parkinsonian gait analyzed by a long-term daily monitoring system. *European Neurology*. 2013;**69**(3):134-141
- [49] Yoneyama M, Mitoma H, Higuma M, Sanjo N, Yokota T, Terashi H. Ambulatory gait behavior in patients with dementia: A comparison with Parkinson's disease. *IEEE Transactions on Neural Systems and Rehabilitation Engineering*. 2016 Aug;**24**(8):817-826
- [50] Yoneyama M, Mitoma H, Hayashi A. Effect of age, gender, and walkway length on accelerometry-based gait parameters for healthy adult subjects. *Journal of Mechanics in Medicine and Biology*. 2015;**16**:1650029
- [51] Yoneyama M, Okuma Y, Utsumi H, Terashi H, Mitoma H. Human turnover dynamics during sleep: Statistical behavior and its modeling. *Physical Review E*. 2014. DOI: DOI 10.1103/PhysRevE.002700
- [52] Higuma M, Sanjo N, Mitoma H, Yoneyama M, Yokota T. Whole-day gait monitoring in patients with Alzheimer's disease: Relationship between attention and gait cycle. *JAD Reports*. 2017. DOI: 10.3233/ADR-170001
- [53] Terashi H, Mitoma H, Yoneyama M, Aizawa H. Relationship between amount of daily movement measured by a triaxial accelerometer and motor symptoms in patients with Parkinson's disease. *Applied Sciences*. 2017;**7**:486
- [54] Iijima M, Mitoma H, Uchiyama S, Kitagawa K. Long-term monitoring gait analysis using a wearable device in daily lives of patients with Parkinson's disease: The efficacy of selegiline hydrochloride for gait disturbance. *Frontiers in Neurology*. 2017;**8**:542
- [55] Morris ME, Ianssek R, Matyas TA, Summers JJ. The pathogenesis of gait hypokinesia in Parkinson's disease. *Brain*. 1994 Oct;**117**(Pt5):1169-1181
- [56] Morris ME, Ianssek R, Matyas TA, Summers JJ. Ability to modulate walking cadence remains intact in Parkinson's disease. *Journal of Neurology, Neurosurgery, and Psychiatry*. 1994 Dec;**57**(12):1532-1534
- [57] Morris ME, Ianssek R, Matyas TA, Summers JJ. Stride length regulation in Parkinson's disease. Normalization strategies and underlying mechanisms. *Brain*. 1996 Apr;**119**(Pt2):551-568

- [58] Hallett M, Khoshbin S. A physiological mechanism of bradykinesia. *Brain*. 1980 Jun; **103**(2): 301-314
- [59] Flowers KA. Visual “closed-loop” and “open-loop” characteristics of voluntary movement in patients with parkinsonism and intention tremor. *Brain*. 1976 Jun; **99**(2):269-310
- [60] Marsden CD, Parkes JD, Quinn N. Fluctuations of disability in Parkinson’s disease: Clinical Aspects. In: Marsden CD, Fahn S, editors. *Movement Disorders*. London, UK: Butterworth Scientific; 1982. pp. 96-112
- [61] Giladi N. Medical treatment of freezing of gait. *Movement Disorders*. 2008; **23**:S482-S488
- [62] Stacy M, Bowron A, Guttman M, Hauser R, Hughes K, Larsen JP, LeWitt P, Oertel W, Quinn N, Sethi K, Stocchi F. Identification of motor and nonmotor wearing-off in Parkinson’s disease: Comparison of a patient questionnaire versus a clinician assessment. *Movement Disorders*. 2005 Jun; **20**(6):726-723
- [63] Stacy M, Hauser R. Development of a patient questionnaire to facilitate recognition of motor and non-motor wearing-off in Parkinson’s disease. *Journal of Neural Transmission*. 2007 Feb; **114**(2):211-217
- [64] Zijlstra W, Hof AL. Assessment of spatio-temporal gait parameters from trunk accelerations during human walking. *Gait & Posture*. 2003 Oct; **18**(2):1-10